

# COLOR ORIGIN OF LAVENDER JADEITE: AN ALTERNATIVE APPROACH

Ren Lu

The market value of jadeite has risen dramatically in recent decades, often rivaling that of fine ruby and sapphire. Understanding the color origin of jadeite and reliably determining treatments have become increasingly important in the trade. This study uses single-crystalline analogs in conjunction with polycrystalline jadeite to examine the color origin of lavender jadeite through quantitative spectroscopy and modern trace-element analytical techniques. Several previously proposed chromophores are assessed for their possible contribution to jadeite coloration. Quantitative analysis confirms that green and lavender colorations are caused by chromium and manganese, respectively. The relative significance of these two chromophores is compared to determine their impact on observable coloration. The findings on color origin are applied to the identification of treated material on the current market.

Jadeite is a highly regarded gemstone, particularly in Asian markets. Some of the finest pieces command premium values, often surpassing those for top-quality ruby, sapphire, and emerald, as evidenced by recent auctions (Leblanc, 2012). At Christie's Hong Kong sale on May 29, 2012, a lavender jadeite bangle fetched US\$453,003.

The value of a gem material largely depends on whether it is of natural, treated, or synthetic origin (figure 1). Gemological testing and detection of color enhancement rely on a clear understanding of color origin. The detection of chromophore(s) appropriate for the observed color is required for a natural color determination.

Trivalent chromium ( $\text{Cr}^{3+}$ ) and iron ( $\text{Fe}^{3+}$ ) have long been known as the source of "emerald" and "grassy" green colors in jadeite, respectively (Harlow and Olds, 1987; Rossman, 1977). Yet the origin of lavender color has been a subject of debate among various studies over the past 30 years. Various chromophores—including single transition metal ions  $\text{Mn}^{3+}$ ,  $\text{Mn}^{2+}$ ,  $\text{Ti}^{3+}$ ,  $\text{Fe}^{3+}$ , and  $\text{V}^{3+}$ , and paired charge-transfer ions  $\text{Fe}^{2+}\text{-Fe}^{3+}$ ,

and  $\text{Ti}^{4+}\text{-Fe}^{2+}$ —have been proposed based on UV-visible spectroscopic data, chemical analyses, and comparisons to similarly colored minerals (Rossman, 1974; Shinno and Oba, 1993; Chen et al., 1999; Ouyang, 2001; Harlow and Shi, 2011).

Quantitative analysis relies on the precise determination of chromophore concentration and the op-

*Figure 1. Most intense lavender-color jadeite has been treated to achieve that saturation of color but this cabochon is natural color. Photo by Tino Hammid/GIA.*



See end of article for About the Author and Acknowledgments.

GEMS & GEMOLOGY, Vol. 48, No. 4, pp. 273–283,  
<http://dx.doi.org/10.5741/GEMS.48.4.273>.

© 2012 Gemological Institute of America

tical path length that light travels through a region of particular absorption characteristics. Such direct and quantitative correlation between proposed chromophores and observed lavender jadeite color has been lacking, however. Three main challenges intrinsic to jadeite have hindered our understanding of the gem's chromophores:

1. The polycrystalline and sometimes near crypto-crystalline nature of the finest jadeite poses fundamental difficulties. In polycrystalline materials, light does not follow a direct path. The path length is not simply the thickness of the material, but rather an indirect and complicated path through all the irregularities of crystal grains.
2. Chromophore characterization has traditionally relied on electron microprobe analysis, which is best suited for major elements but insufficient for detecting trace elements. Yet chromophores are often trace elements at parts-per-million (ppm) levels, rather than main elements at percent (parts-per-hundred) levels. For instance, a trace amount of chromium at only a few hundred ppm can produce appreciable colors in ruby (McClure 1962; Eigenmann et al., 1972; and the author's recent analysis of hundreds of ruby samples) or green jadeite (analysis presented below). Similarly, a few tens of ppm of beryllium will readily alter the color of sapphire (Emmett et al., 2003). Thus the true chromophore(s) responsible for the observed color may not be correctly identified due to limited sensitivity of analytical techniques.
3. Multiple transition metal ions or pairs are known to produce broad absorption bands in the same general region (near 550–650 nm) responsible for a lavender color.

This study takes a completely different approach to addressing color origin in lavender jadeite by quantitatively analyzing high-quality single-crystals of closely matched materials.

Spodumene and jadeite share closely matched crystallographic structures and optical and spectroscopic properties. Similar to jadeite, spodumene is available in both green (hiddenite) and pink/lavender (kunzite) color. Unlike jadeite, which is polycrystalline and rarely exhibits large crystals, high-quality single crystals of spodumene are widely available, which facilitates quantitative spectroscopic and trace-element (chromophore) analysis. The quantita-

tive results are consequently instructive to the analysis of color origin and to determining enhancement of lavender jadeite

In terms of technical approach, two key components of this study are quantitative absorption spectroscopy and trace-element analysis at the parts-per-million level (Box A). This is achieved through laser ablation–inductively coupled plasma–mass spectrometry (LA-ICP-MS), a technique that has become practical only in recent years. These mass spectrometers provide point-by-point chemical analysis with micrometer-size spatial resolution and concentrations better than parts-per-million, which can be fully correlated to quantitative absorption spectroscopy in color analysis.

## MATERIALS AND METHODS

Nine natural jadeite slabs ranging from ~16 to 88 ct with well-known provenance (Nant Maw mine 109, Myanmar; Kotaki-Gawa Itoigawa, Japan; and near Saltan and La Ensenada, Guatemala) were provided by Dr. George Harlow of the American Museum of Natural History in New York. These materials were mostly whitish, with zones of pinkish lavender (Burmese) and bluish lavender (Japanese and Guatemalan) colors. Sixteen faceted pieces of known impregnated and/or color-enhanced lavender and purplish jadeite materials were provided by Chinese dealers. To test the alternative approach to establishing color origin, three centimeter-size gem-quality natural crystals of spodumene (hiddenite and kunzite varieties) from Afghanistan were obtained from GIA collections.

**UV-Visible Spectroscopy.** Jadeite and spodumene samples were prepared as wafers with parallel polished surfaces and various thicknesses. For single crystals of spodumene, three sets of parallel polished surfaces with maximum pleochroic colors were prepared using a custom-built optical orientation device. UV-visible spectra were collected with a Perkin-Elmer PE950 spectrometer equipped with mercury and tungsten light sources, and photomultiplier tube/PbS detectors that were built into an integrating sphere. A custom-made sample holder specially developed for quantitative analysis was used to ensure the precise positioning of the sampling area in a 3 mm diameter window. The same sampled area was further analyzed by LA-ICP-MS, particularly for trace-element composition to correlate spectral features with potential chromophores. Polarized spectra

## BOX A: QUANTITATIVE CHROMOPHORE ANALYSIS FROM SPECTROSCOPY AND TRACE-ELEMENT CHEMISTRY

The combination of UV-visible absorption spectroscopy and chemical analysis allows us to determine the chromophore(s) that cause the observed color. Figure A-1 illustrates how this is accomplished. Absorption is proportional to the concentration of absorbers through which light passes (known as the Beer-Lambert law). A few relatively simple mathematical steps will lead to the following:

$$\text{Equation 1} \quad \sigma = \frac{A}{Nd} * \ln 10$$

$$\text{Equation 2} \quad A = A_0 \frac{Nd}{N_0 d_0}$$

where:

A is absorbance

$\sigma$  is the absorption cross section

N is the concentration of absorbers

d is the thickness the light path length

and symbols with the subscript "0" are sets of known values of these parameters.

Absorption cross section is a constant for a particular chromophore. Consequently, absorption for any chromophore concentration and sample thickness can be predicted from the relationships above. For instance, more saturated color (and correlating absorbance A) can be achieved by either increasing chromophore concentration (N) or thickness of sample (d).

In this sample for ruby (personal data), a known set of values  $A_0$ ,  $N_0$ , and  $d_0$  are established from the UV-visible absorption spectrum, LA-ICP-MS analysis, and measure-

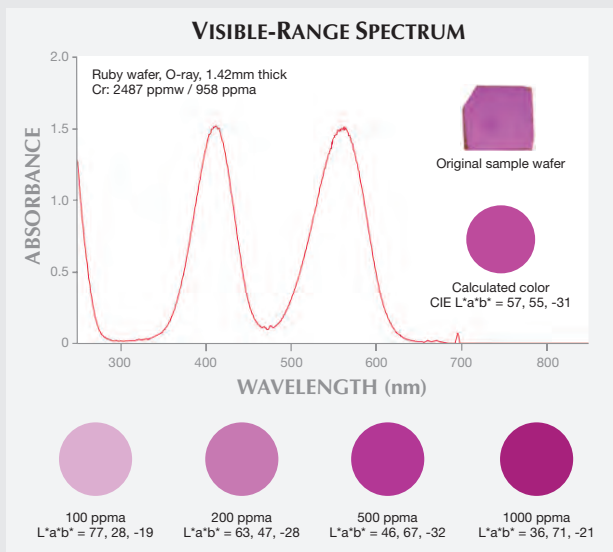


Figure A-1. This visible-range spectrum depicts the determination of chromophore (Cr) in a ruby sample. The color circles (below the spectrum) demonstrate coloration for rubies with various Cr concentrations for a 5 mm path length. Rubies with twice the Cr concentration and half the path length appear the same as 200 ppma and 2.5 mm path length.

ment of thickness, respectively. Color coordinates (CIE  $L^*a^*b^*$ ) can be calculated from absorbance/transmittance, and the color of the sample is quantitatively reproduced using software such as Adobe Photoshop.

were collected in the 200–1400 nm range with a 0.65 nm spectral resolution at a scan speed of 96 nm/min.

Quantitative UV-visible spectroscopic measurement for colors relies on correctly identifying the spectral baseline. Internal scatter in polycrystalline aggregates offsets and distorts the baseline, particularly in the UV spectral region. The spectral baseline was corrected by subtracting spectral offset at or beyond 1000 nm, where the chromophore's features were insignificant or nonexistent.

**LA-ICP-MS Analysis.** Detailed chemical compositions were obtained in the same region characterized by spectroscopy. A ThermoFisher X-series II mass spectrometer from Electro Scientific Industries, Inc. coupled with a deep UV laser at 213 nm excitation

was used in the trace-element analysis. NIST (National Institute of Science and Technology) glass standards SRM 610 and 612 were used for internal calibration (<http://www.nist.gov/srm/>). Ablation conditions were 7 Hz repetition rate, 7 J/cm<sup>2</sup> fluence, and a laser spot size of 40  $\mu$ m.

### RESULTS AND DISCUSSION

**Gemological Observation.** Gemological properties of natural, treated, and synthetic jadeite have been extensively documented (e.g., Koivula, 1982; Nassau and Shigley, 1987). Details and additional references can be found therein and are not discussed here.

Within the gem trade, lavender jadeite loosely refers to a broad range of colors from pinkish, purplish, violetish, to bluish hues. Of the samples col-

lected for this study, the Japanese and Guatemalan jadeite displayed only bluish to bluish green coloration, with virtually no lavender color. The Burmese material showed more pinkish and purple hues with a whitish matrix. Furthermore, lavender regions exhibited a more granular texture, sometimes with large and transparent elongated or orthogonal crystals in concentrated colors (figure 2).

The warmer-toned, more pinkish Burmese samples were inert or showed a very weak reddish reaction under long-wave (~365 nm) and short-wave (~254 nm) UV radiation. The more bluish Japanese and Guatemalan samples exhibited no visible reaction under long- and short-wave UV.

**Jadeite and Spodumene as Close Analogs.** Jadeite ( $\text{NaAlSi}_2\text{O}_6$ ) and spodumene ( $\text{LiAlSi}_2\text{O}_6$ ) share closely matched mineralogical and gemological properties. These properties include Mohs hardness (6.5–7), RI (1.66 vs. 1.66–1.68), and SG (3.34 vs. 3.18). Pure jadeite and spodumene with this ideal chemical composition are colorless.

As members of the pyroxene mineral group, both jadeite and spodumene share the monoclinic  $C2/c$  symmetry and have similar structures (Cameron et al., 1973; see figure 3). The largely distorted octahedral M2 site is occupied by Na (jadeite) or Li (spodumene). The  $\text{SiO}_4$  tetrahedral site is likely not involved in producing colors through substitution by

Figure 2. Saturated lavender colors are often associated with a granular texture, sometimes with orthogonal crystals, as in this Burmese lavender jadeite. The color of these crystals varies noticeably from purplish to bluish when illuminated by directional lighting at various angles. The matrix is mostly whitish. Photo by R. Lu; image width ~12 mm.

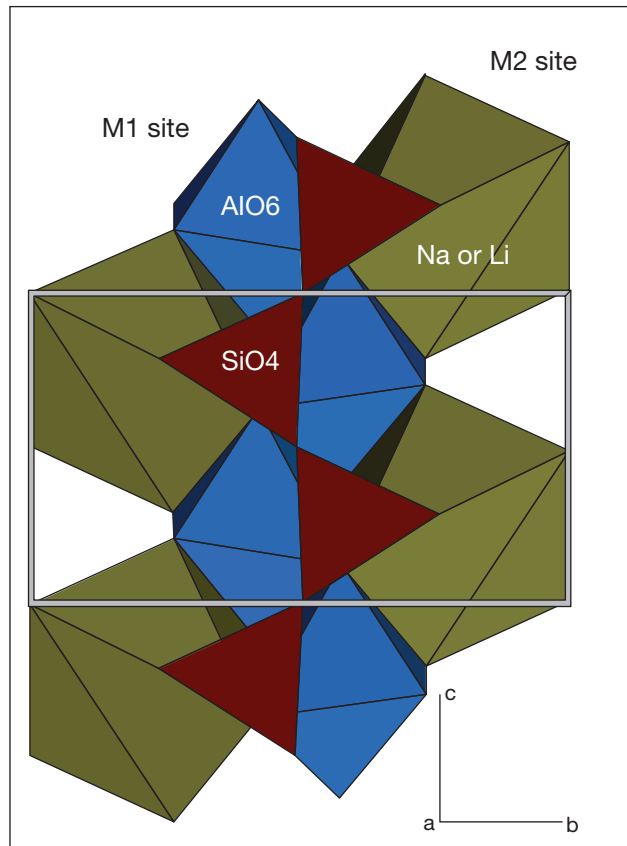


Figure 3. This view of the crystal structure of jadeite and spodumene illustrates the basic building blocks:  $\text{AlO}_6$  octahedra and  $\text{SiO}_4$  tetrahedra, and their geometric relationships (based on structural refinement data of Cameron et al., 1973). The crystallographic orientation is shown in the lower right corner projected down the  $a$ -axis.

trace elements such as transition metals. The slightly distorted M1 octahedral site is occupied by Al or substituted by chromophores such as Cr (which causes green color) supported by the color origin in chromium end-member kosmochlor ( $\text{NaCrAl}_2\text{O}_6$ ) (White et al., 1971) and by the current data comparing green jadeite and hiddenite (discussed below). These octahedra are edge-shared, facilitating possible paired substitutions by chromophore ions in neighboring octahedra. Furthermore, there is only a ~1% difference in the average  $\langle \text{Al-O} \rangle$  distance in the aluminum octahedral site between jadeite and spodumene. Consequently, chromophores substituted into the Al site are expected to present similar UV-visible absorption features.

The following analysis of chromophore chemistry and absorption spectroscopy indicates the chromophore similarities between green jadeite and hiddenite, and between lavender jadeite and kunzite.

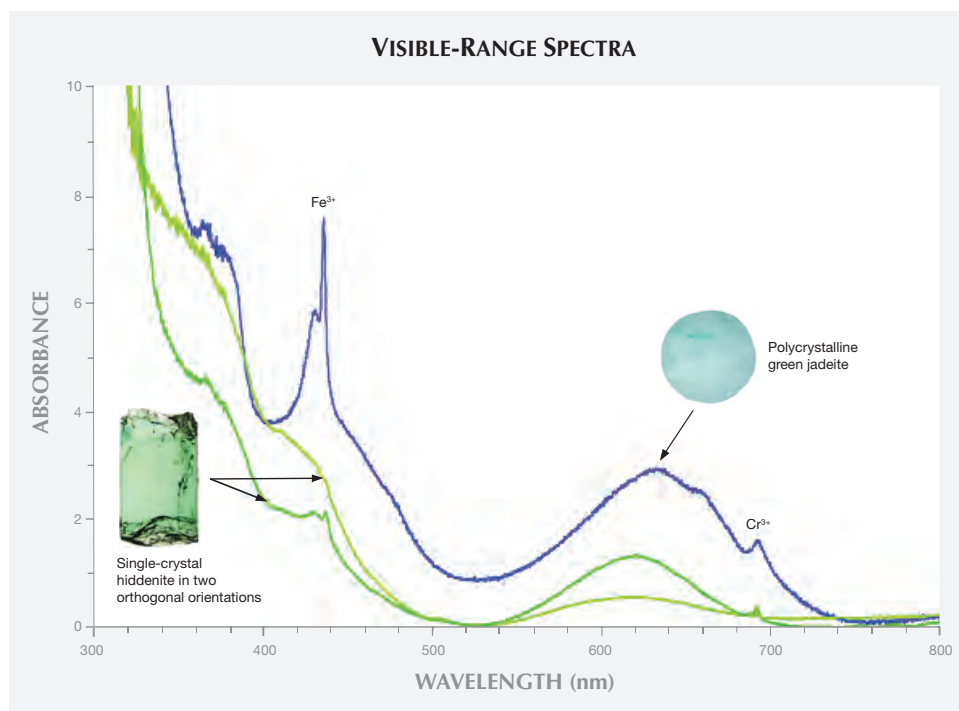


Figure 4. The UV-visible spectra of green jadeite and green spodumene (hiddenite) exhibit closely matched absorption features. Hiddenite spectra were collected from two orthogonal orientations, with polarized light demonstrating noticeable pleochroism in single crystals. The visible difference in green saturation is mostly due to the disparity in sample thickness (~0.94 mm for jadeite and ~2.7 mm for hiddenite) rather than a difference in chromium concentration (see table 1). The spectra are for element concentrations listed on table 1.

**UV-Visible Spectroscopy.** Correlating an observed color to a specific chromophore requires precise measurement of absorption features through a known optical path in the UV-visible spectrum as well as chemical analysis of the chromophore's concentration. High-quality single-crystal spodumene presents an ideal opportunity for quantitative understanding of color origin in polycrystalline jadeite, which is complicated by textural and chemical variations.

The UV-visible spectra of hiddenite show features corresponding with those of chromium-bearing green jadeite (figure 4). The characteristic 437 nm absorption band of  $Fe^{3+}$ , commonly present in natural jadeite with various green hues, is about 1 nm higher in hiddenite. The narrow 691 nm absorption band of  $Cr^{3+}$  is virtually the same in both minerals.

Pleochroic colors from yellowish green to bluish green, visually observable with a handheld dichroscope, were quantitatively reproduced in single-crystal spectra of hiddenite. Figure 4 shows the variation in green saturation and hue observed approximately along two principal optical orientations with the maximum contrast in hue and saturation. The crystal orientation device used in this current study is being redesigned to allow analysis of fully oriented crystals in all three principal optical orientations of biaxial crystals such as spodumene.

In general, pleochroism is not observed among randomly oriented polycrystalline jadeite, particularly fine-grained, high-quality specimens.

UV-visible spectra of kunzite (figure 5) showed strong pleochroism ranging from variously saturated pink to a bluish hue dominated by broad bands above ~500 nm in the three orthogonal directions.

An aggregate of randomly oriented crystals of lavender jadeite showed a combination of pink and blue (purplish) hues. A large variation in both saturation and hue is commonly observed with direc-

## In Brief

- The color origin (natural or otherwise) of lavender jadeite is an essential aspect of its commercial value.
- While detecting the color-causing elements of polycrystalline jadeite is difficult, the single-crystal analog spodumene has very similar properties and lends itself to quantitative analysis.
- LA-ICP-MS analysis mapped to quantitative spectroscopy confirms that manganese and chromium are responsible for lavender and green colorations in jadeite, respectively.
- A reddish fluorescence reaction to deep UV radiation is a likely indication of the presence of manganese, and of natural color in lavender jadeite.

tional illumination (such as a fiber-optic light) at different angles. The variation is more pronounced in single-crystal kunzite and in polycrystalline lavender jadeite with coarse grains (figure 2).

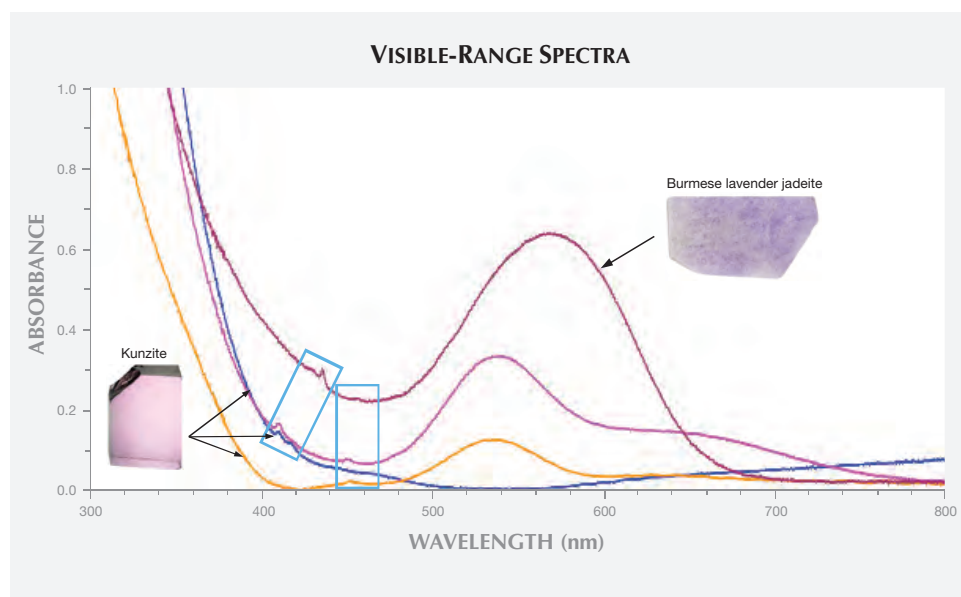


Figure 5. As these UV-visible absorption spectra demonstrate, polycrystalline Burmese lavender jadeite and single-crystalline pink spodumene (kunzite) share similar weak narrow bands (blue boxes) between 400 and 460 nm and similar broad bands above 500. The single-crystal kunzite spectra were collected from the three orthogonal orientations that displayed the most pleochroism, ranging from pink (pink line) to light pink (orange line) and very light blue-green (blue line).

A larger difference was observed in the iron-related narrow bands between kunzite and lavender jadeite (blue boxes in figure 5) than between hiddenite and green jadeite. The source of this large difference is unknown and requires further study. One possible source might be the interaction between neighboring Mn and Fe replacing Al.

**Chromophore Analysis.** Trace elements were thoroughly analyzed for the chromophores that cause lavender and other hues in jadeite. These included the transition-metal ions proposed by previous studies, listed in table 1. The polycrystalline jadeite samples showed variation in chromophore concentration that correlated to visible differences in color saturation. The chromophore concentration was averaged over 30 laser ablation spots across a 3 mm circular area through which spectroscopic characterization was performed.

Element concentration was measured by LA-ICP-MS analysis of jadeite and spodumene samples (transition metals V and Co were below detection limits and not listed). Concentrations for polycrystalline jadeite samples with various lavender saturations were averaged over 30 analysis spots. For Burmese lavender jadeite, Mn concentrations ranged from as low as 4 ppma for whitish matrix to as high as 195 ppma in more saturated lavender areas (further evidenced by the fluorescence image in figure 10b).

For kunzite, manganese is clearly the only available chromophore for the pink/lavender coloration. For Burmese lavender jadeite, similarly, iron below

100 ppma is insignificant in producing any color, and consequently the only chromophore is manganese.

**Consideration of Ionic Structure.** Valence and size of ions play a critical role in their incorporation as possible chromophores. Isovalent ions  $Mn^{3+}$ ,  $Cr^{3+}$ ,  $Fe^{3+}$ ,  $Co^{3+}$ , and  $V^{3+}$  are charge-balanced, and their ionic radii fall closely to that of  $Al^{3+}$  in six-fold coordinated octahedral sites, facilitating substitution into the Al octahedral site (figure 6). Cobalt and vanadium are not shown or discussed further because they are absent in lavender jadeite (table 1).

Manganese is virtually the only chromophore in pink spodumene and clearly responsible for its coloration. Both  $Mn^{2+}$  and  $Mn^{3+}$  can occur in six-fold octahedral coordination, and they are known to cause pink or red colors in minerals (e.g., rhodonite, andalusite, grossular, morganite, red and pink tourmaline, and kunzite).

For consideration of ionic radii, isovalent  $Mn^{3+}$  is the preferred chromophore because its ionic charge and size match those of  $Al^{3+}$ . Aliovalent  $Mn^{2+}$  has a noticeably larger ionic size than  $Al^{3+}$  and requires additional charge compensation to fit into the  $Al^{3+}$  octahedral site. It is thus a less likely candidate for the lavender or pink hue in jadeite and spodumene.

Unlike  $Mn^{3+}$ ,  $Mn^{2+}$  tends to produce relatively weak absorption bands, attributed in the technical literature to weak oscillator strength or low cross-section involving spin-forbidden transitions, when coordinated to oxygen ligands ( $Mn^{2+}-O^{2-}$ ) (Burns, 1993, p. 217). Consequently, the divalent  $Mn^{2+}$  pro-

**TABLE 1.** Elemental concentrations in ppma.

Name	<sup>55</sup> Mn	<sup>53</sup> Cr	<sup>57</sup> Fe	<sup>47</sup> Ti
Lavender jadeite (Burmese)	99	0	76	0
Green jadeite (avg)	41	268	1528	48
Bluish jadeite Japan	10	0	1011	586
Bluish jadeite Guatemala	1	0	73	356
Kunzite	127	0	0	5
Hiddenite	374	21	1676	27
<b>Treated materials</b>				
Lavender jadeite B+C type (sample A)	5	0	404	13
Lavender jadeite B+C type (sample B)	15	0	465	12
Lavender jadeite dyed bicolored ring	15	0	451	11
Detection limit	0.3	1	16	1

duces near-colorless or weak coloration, as opposed to the more effective trivalent Mn<sup>3+</sup> chromophore. At the low Mn level of 100 ppma (table 1), the pink and lavender coloration in kunzite and lavender jadeite should correlate to their Mn<sup>3+</sup> concentration.

For the same reason, trivalent Fe<sup>3+</sup>, which shares the same electronic structure as Mn<sup>2+</sup>, is a weak chromophore and only produces noticeable color at high concentrations. For instance, a saturated yellow color in sapphire requires at least ~1000 ppma Fe<sup>3+</sup> (author's personal data). This is important in understanding the relatively weak contribution of Fe<sup>3+</sup> to coloration.

The kunzite and Burmese lavender samples showed pink/lavender colors owing to their desirable combination of appreciable Mn and the absence of Fe. By comparison, the lack of appreciable Mn in bluish Japanese and Guatemalan materials explains their lack of a pinkish color component.

**Other Candidate Chromophores.** Three other transition metal ions—titanium (Ti), vanadium (V), and cobalt (Co)—are effective chromophores and may produce broadband absorption features that overlap with those from Mn in the 600 nm region (Wood and Nassau, 1968; Shigley and Stockton, 1984). But in Burmese samples with a warm pinkish lavender color, the concentrations of Ti, V, and Co are too low to cause any noticeable color.

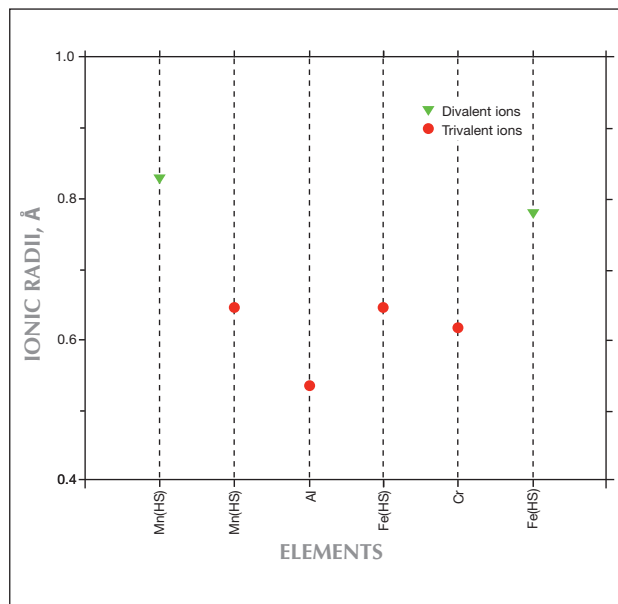
Furthermore, incorporation of chromophores in minerals depends on their availability in nature and the physical and chemical compatibility of the sub-

stituting ion (e.g., Al<sup>3+</sup> in jadeite). A mechanism for chromium incorporation in green jadeite has been proposed based on petrological and chemical analysis (e.g., Shi et al., 2005; Harlow et al., 2007). Information about the petrological source and incorporation of Mn in lavender jadeite is still lacking, however.

**Comparison of Chromophore Effectiveness.** To better understand jadeite coloration, it is worthwhile to compare the effectiveness of chromophores Cr (green) and Mn (lavender). As shown in table 1, hiddenite contains an appreciable amount of Mn in addition to Cr. Yet chromium features dominate hiddenite's absorption spectrum.

For a given sample thickness, absorbance in the UV-visible spectrum is proportional to the concentration of the absorbing element in the part of the stone where light passes through according to the Beer-Lambert law. For a 5 mm thickness, UV-visible spectra were calculated for various chromophore concentrations based on experimentally collected hiddenite and kunzite absorption spectra. Figure 7 compares the effectiveness of Cr and Mn as chromophores.

Figure 6. Ionic radii of trivalent ions such as Mn, Fe, and Cr (isovalent to Al<sup>3+</sup>, in solid circles) closely match those of Al<sup>3+</sup> and can readily replace Al<sup>3+</sup> as chromophore ions. Divalent ions (aliovalent to Al<sup>3+</sup>, in solid triangles) are less suited in terms of size and charge balance. The label "HS" represents high-spin configuration. Data for ionic radii of six coordinated ions are based on Shannon (1976).



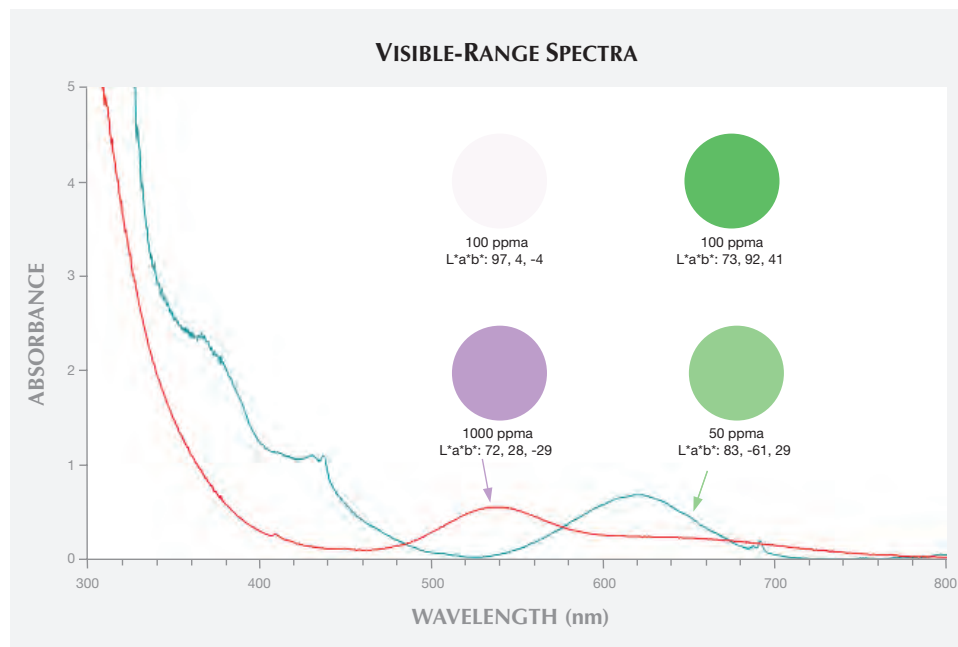


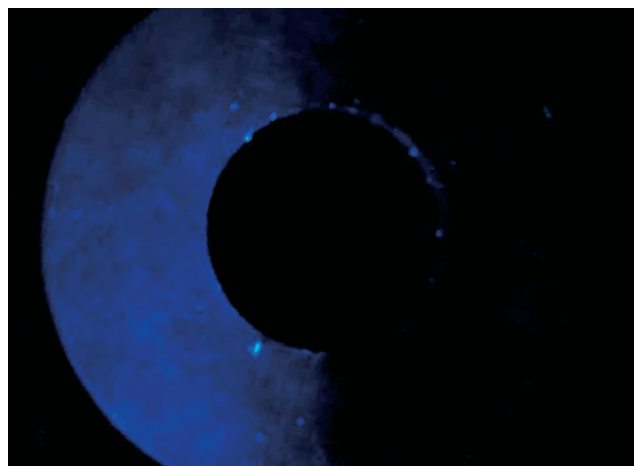
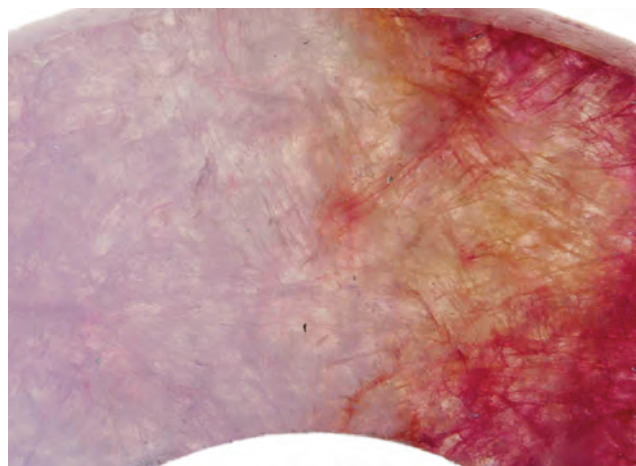
Figure 7. Absorption spectra and their corresponding color circles compare the chromophore effectiveness of Mn and Cr (5 mm path length). The lower circles represent similar color saturations for lavender and green jadeite. The upper circles demonstrate the color saturations (and absorbance) for matching chromophore concentrations of 100 ppma. A relatively low Mn concentration (e.g., < 100 ppma) would be virtually colorless. The CIE  $L^*a^*b^*$  color coordinates are presented with specification of CIE Adobe RGB1998 and D55.

The implication of figure 7 is that pink/purple color from manganese only becomes noticeable at very high concentrations and in the absence of the much more effective chromophore chromium. This result is expected to be at least qualitatively true for Cr-bearing green jadeite and Mn-bearing lavender jadeite. Hatipoglu et al. (2012) recently reported Mn levels as high as 1540 ppmw (565 ppma) in deep lavender/purple jade from Turkey, in general agreement with this study.

**Detecting Dyed Lavender Jadeite.** Earlier dyed jadeite tended to show obvious color concentrations and an orangy color reaction under long-wave UV radiation (Koivula, 1982). These characteristics are often much less pronounced in the dyed material currently on the market, particularly fine-textured specimens (figure 8).

UV-visible spectra of dyed lavender/purple jadeite generally show broad absorption bands near 530 nm, but multiple broad bands are possible, presumably due to variations in the dyes (figure 9). These dye materials

Figure 8. This dyed bicolored ring shows easily identifiable color concentrations in grain boundaries (left) but exhibits no reaction to long-wave UV radiation (right). The width on the left image is ~5.5 mm, and the outer diameter of the ring is 11 mm. Photos by Jian Xin (Jae) Liao.



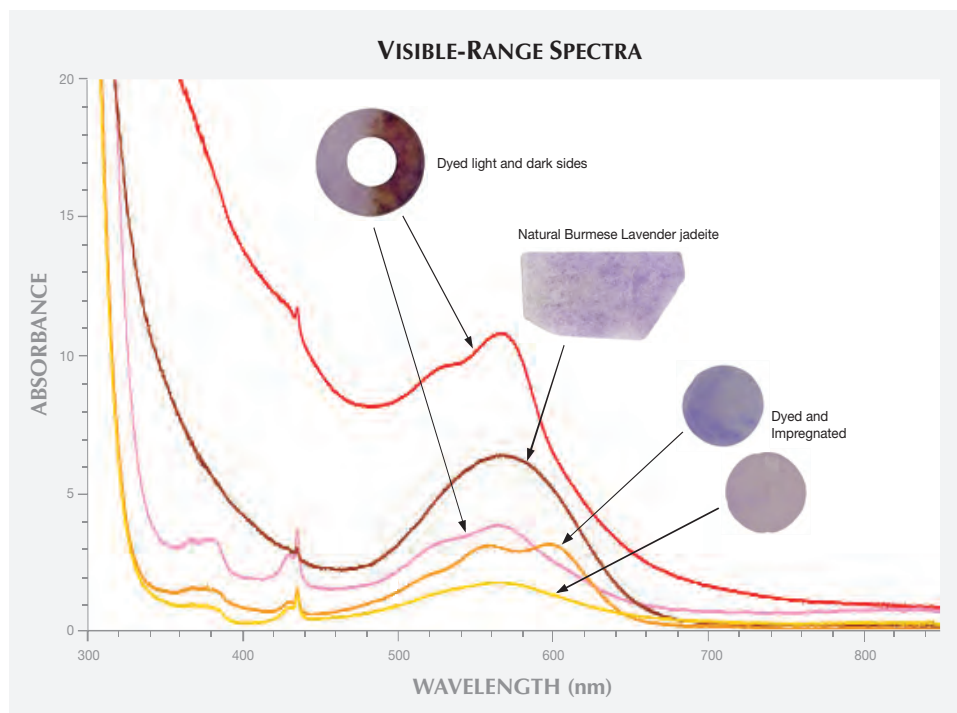


Figure 9. The UV-visible spectra of dyed jadeite show single or multiple broad bands between 500 and 650 nm that generally overlap with the broad band from Mn near 570 nm observed in untreated Burmese material. The narrow  $\text{Fe}^{3+}$  features near 437 nm in the treated material are more pronounced due to higher iron concentration.

are likely of organic origin and are not detected by LA-ICP-MS trace element analysis. When the concentration of natural Mn is too low to produce a saturated lavender color, a dye is introduced. Dye-related broad bands are superimposed with the Mn broad band near 570 nm to produce multiple bands.

A pronounced  $\text{Fe}^{3+}$  absorption in the blue spectral region near 437 nm indicates a relatively high iron concentration, which typically produces an undesired yellow-brown overtone. A combination of strong  $\text{Fe}^{3+}$  bands and multiple broad bands in the 550–650 nm region would be unlikely to yield a lavender color.

Additional tests were performed with a DTC DiamondView to explore potential techniques for identifying color origin and treatment. Under the strong short-wave UV radiation of the DiamondView (at wavelength shorter than ~230 nm), the Burmese samples showed an intense reddish reaction correlating to higher Mn concentrations, up to 195 ppm (figure 10B, also refer to table 1). The kunzite crystal exhibited a pinkish color (figure 10A) due to a relatively lower Mn concentration (127 ppm). Dyed lavender jadeite with various pinkish or purplish colors did not show the reddish reaction observed in Burmese samples under the DiamondView (figure

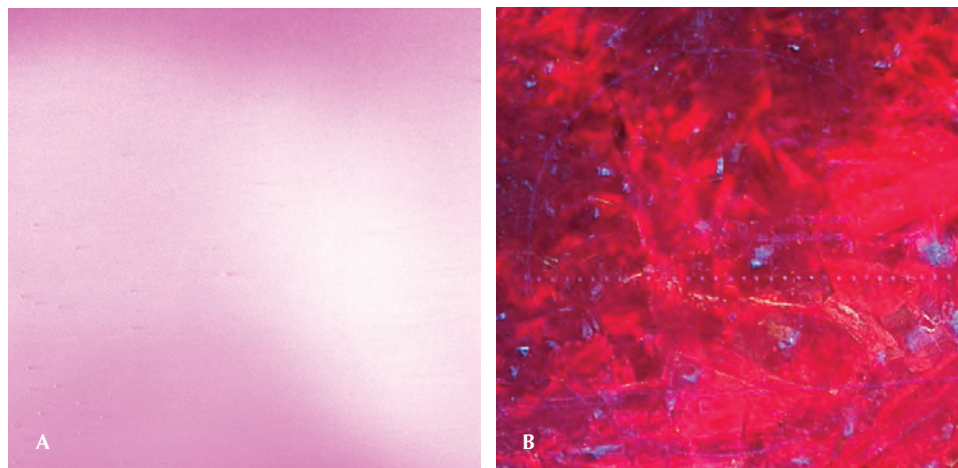


Figure 10. DiamondView images show reactions in Mn-bearing single-crystal kunzite (A) and polycrystalline Burmese lavender jadeite (B). The row of tiny dots (0.1 mm apart) in the center of image B is from LA-ICP-MS analysis, and the bluish speckles are due to reflection. Image widths ~5 mm. More saturated reddish colors (B) correlate to higher Mn concentrations in jadeite. Photos by R. Lu.

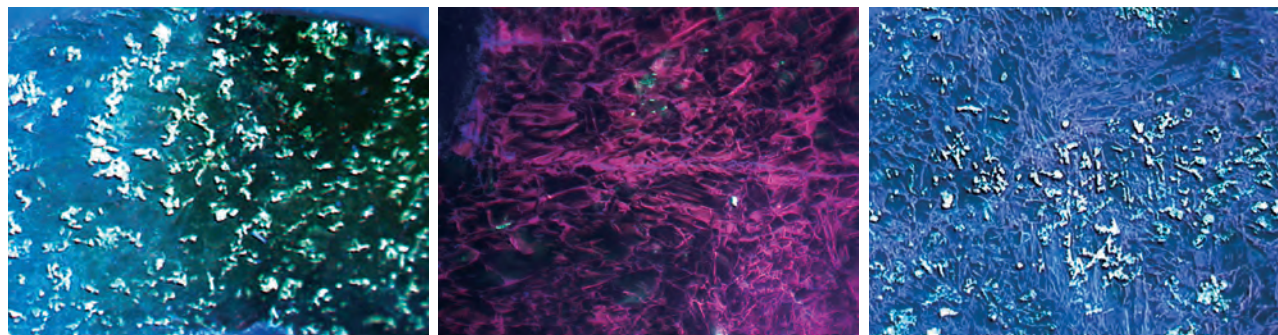


Figure 11. DiamondView images of a dyed bicolored ring (left) and two dyed and impregnated purplish lavender samples (center and right) show no reaction or a weak purplish and bluish reaction. The reddish reaction seen in natural Mn-bearing Burmese samples and the well-known orange “dye reaction” were not observed in the dyed materials currently on the market. Image widths ~5.5 mm. Photo by R. Lu.

11). The same observation was performed on bluish natural jadeite materials from Japan and Guatemala. Due to the absence of Mn in these samples, only bluish or greenish reactions were observed.

## CONCLUSIONS

Nature provides high-quality single-crystal spodumene in both green and pink varieties. Their properties closely match those of jadeite, providing a framework for an alternative approach to the quantitative study of chromophore species in polycrystalline jadeite.

The current quantitative chromophore analysis is achieved by employing the unique high spatial resolution of LA-ICP-MS analysis of trace elements which is precisely mapped to quantitative spectroscopy. This technique is applicable to studies of a wide range of gemological materials.

This study confirms that manganese and chromium are responsible for lavender and green colorations

in jadeite, respectively. Furthermore, chromium is at least two orders of magnitude more effective in producing green coloration than manganese for lavender of similar saturation. The sharp difference in chromophore effectiveness between chromium and manganese dictates that green coloration is more readily observable than lavender. Consequently, a natural lavender color is not expected to be associated with a high chromium concentration within the same sample area.

Reddish (or blue/green) fluorescence reaction from deep UV radiation is a likely indication of the presence (or absence) of manganese, and of natural color in lavender jadeite. Further validation of this result will benefit color origin determination in jadeite testing. In combination with this fluorescence reaction, the detailed structure of absorption bands near 570 nm in UV-visible spectra is helpful in detecting dye treatment.

### ABOUT THE AUTHOR

Dr. Lu is a senior scientist at GIA's New York laboratory.

### ACKNOWLEDGMENTS

Dr. George Harlow (American Museum of Natural History, New York) graciously provided natural lavender jadeite materials mostly collected from his personal trips to Myanmar, Japan, and

Guatemala. Terri Ottaway (GIA, Carlsbad) kindly selected gem-quality natural single crystals of hiddenite and kunzite spodumene. Sincere thanks go to Dr. Wuyi Wang (GIA, New York) for obtaining known treated samples from dealers in the Hong Kong and mainland Chinese markets. The author would like to sincerely thank the manuscript's three reviewers for their constructive comments.

## REFERENCES

Burns R.G. (1993) *Mineralogical Applications of Crystal Field Theory*, 2nd ed. Cambridge University Press, New York, p. 523.  
Cameron M., Sueno S., Prewitt C.T., Papike J.J. (1973) High-tem-

perature crystal chemistry of acmite, diopside, hedenbergite, jadeite, spodumene, and ureyite. *American Mineralogist*, Vol. 58, pp. 594–618.

- Chen B. Qiu Z. Zhang X. (1999) Preliminary study on the mineralogical characters of lavender jadeite jade. *Journal of Gems and Gemmology*, Vol. 3, No. 1, pp. 35–39 (in Chinese).
- Eigenmann K., Kurtz K., Günthard H.H. (1972) The optical spectrum of  $\alpha\text{-Al}_2\text{O}_3\text{:Fe}^{3+}$ . *Chemical Physics Letters*, Vol. 13, No. 1, pp. 54–57.
- Emmett J.L., Scarratt K., McClure S.F., Moses T., Douthit T.R., Hughes R., Novak S., Shigley J.E., Wang W., Bordelon O., Kane R.E. (2003) Beryllium diffusion of ruby and sapphire. *G&G*, Vol. 39, No. 2, pp. 84–134, <http://dx.doi.org/10.5741/GEMS.39.2.84>.
- Harlow G.E., Olds E.P. (1987) Observations on terrestrial ureyite and ureyitic pyroxene. *American Mineralogist*, Vol. 72, pp. 126–136.
- Harlow G.E., Shi G.H. (2011) An LA-ICP-MS study of lavender jadeite from Myanmar, Guatemala, and Japan. *G&G*, Vol. 47, No. 2, pp. 116–117.
- Harlow G.E., Sorensen S.S., Sisson V.B. (2007) Chapter 7. Jade, In L.A. Groat, ed., *The Geology of Gem Deposits*, Short Course Handbook Series, Vol. 37, pp. 207–254.
- Hatipoglu M., Basevirgen Y., Chamberlain S.C. (2012) Gem-quality Turkish purple jade: Geological and mineralogical characteristics. *Journal of African Earth Sciences*, Vol. 63, pp. 48–61.
- Koivula J.I. (1982) Some observations on the treatment of lavender jadeite. *G&G*, Vol. 18, No. 1, pp. 32–35, <http://dx.doi.org/10.5741/GEMS.18.1.32>.
- Leblanc D. (2012) Color stays high at spring and summer auctions. *InColor*, No. 20, pp. 62–67.
- McClure D.S. (1962) Optical spectra of transition-metal ions in corundum. *Journal of Chemical Physics*, Vol. 36, No. 10, pp. 2757–2779.
- Nassau K., Shigley J.E. (1987) A study of the General Electric synthetic jadeite. *G&G*, Vol. 23, No. 1, pp. 27–35, <http://dx.doi.org/10.5741/GEMS.23.1.27>.
- Ouyang Q. (2001) Characteristics of violet jadeite jade and its coloration mechanism. *Journal of Gems and Gemmology*, Vol. 3, No. 1, pp. 1–6 (in Chinese).
- Rossman G.R. (1974) Lavender jade. The optical spectrum of  $\text{Fe}^{3+}$  and  $\text{Fe}^{2+} \rightarrow \text{Fe}^{3+}$  intervalence charge transfer in jadeite from Burma. *American Mineralogist*, Vol. 59, pp. 868–870.
- Shannon R.D. (1976) Revised effective ionic radii and systematic studies of interatomic distances in halides and chalcogenides, *Acta Crystallographica Section A*, Vol. 32, Part 5, pp. 751–767, <http://dx.doi.org/10.1107/S0567739476001551>.
- Shi G.H., Stöckhert B., Cui W.Y. (2006) Texture and composition of kosmochlor and chromian jadeite aggregates from Myanmar: Implications for the formation of green jadeite. *G&G*, Vol. 42, No. 3, pp. 150–151.
- Shigley J.E., Stockton C.M. (1984) “Cobalt-blue” gem spinels. *G&G*, Vol. 20, No. 1, pp. 34–41, <http://dx.doi.org/10.5741/GEMS.20.1.34>.
- Shinno I., Oba T. (1993) Absorption and photo-luminescence spectra of  $\text{Ti}^{3+}$  and  $\text{Fe}^{3+}$  in jadeites. *Mineralogical Journal*, Vol. 16, No. 7, pp. 378–386, <http://dx.doi.org/10.2465/minerj.16.378>.
- White W.B., McCarthy G.J., Scheetz G. E. (1971) Optical spectra of chromium, nickel and cobalt-containing pyroxenes, *American Mineralogist*, Vol. 56, pp. 72–89.
- Wood D.L., Nassau K. (1968) The characterization of beryl and emerald by visible and infrared absorption spectroscopy. *American Mineralogist*, Vol. 53, pp. 777–800.

# GEMS & GEMOLOGY®

## HAS TURNED A NEW PAGE

Your trusted resource for the most reliable research on diamonds and colored stones is now available for iPad.

- Peer-reviewed research
- Groundbreaking discoveries
- Latest gem news
- Superb photography
- Interviews with industry experts, videos, slideshows, and much more...



**Free iPad App Available Now!**

To download, search *Gems & Gemology* in the iPad App Store.



**GIA®**

World Headquarters  
The Robert Mouawad Campus  
5345 Armada Drive  
Carlsbad, CA 92008  
[www.gia.edu](http://www.gia.edu)